Characterization of Complex Formation by Humanized Anti-IgE Monoclonal Antibody and Monoclonal Human IgE

Jun Liu,[‡] Philip Lester,[§] Stuart Builder,[§] and Steven J. Shire*,[‡]

Pharmaceutical Research and Development and Recovery Process Research and Development, Genentech, Inc., South San Francisco, California 94080

ABSTRACT: The interaction of human IgE with high-affinity IgE F_c receptors on cells of the immune system plays an essential role in the type I hypersensitivity reaction. A proposed therapy is to use an anti-IgE monoclonal antibody to block the binding of IgE to its high-affinity receptor on mast cells and basophils, thus preventing subsequent release of the inflammatory agents after exposure to allergen. We report here the solution characteristics of immune complexes formed by a humanized anti-IgE monoclonal antibody (rhuMAb E25) and IgE using sedimentation analysis and size exclusion chromatography. We demonstrate that the rhuMAb E25 is able to form a variety of complexes with IgE at different molar ratios. The largest complex was identified by sedimentation equilibrium analysis as a heterohexamer with very high stability. The intermediate complex formed when one of the interacting components is in large molar excess appears to have a trimeric structure. The high-affinity interaction of rhuMAb E25 and IgE has also been confirmed. Furthermore, by using hydrodynamic modeling, we show that the largest complex may be represented by a cyclic structure.

Human IgE plays a central role in type I hypersensitivity reactions, such as asthma, eczema, and hay fever. Following the initial contact with allergen, the local B cells, stimulated by the signal from the antigen-presenting cells and T_H cells, recognize the appropriate epitopes via specific cell surface receptors and produce specific IgE antibodies. These antibodies bind to the high-affinity F_c receptors ($F_c \epsilon RI$)[1] on basophils in circulation or mast cells in tissues. Subsequent reexposure to the multivalent allergen cross-links the surface IgE and the underlying $F_c \epsilon RI$, thereby triggering the release of histamine, leukotriene, and other intracellular mediators. These pharmacologically active mediators then increase vascular permeability, contraction of vascular smooth muscle, and emigration of neutrophils and monocytes from blood vessels, leading to a variety of symptoms of allergy (Roitt et al., 1989).

Most of the currently available pharmacotherapies are focusing on the later stages of this cascade by using either antagonists of active mediators or mast cell stabilizers. These treatments usually require highly specific antagonists for each mediator without addressing the root of the problem. A proposed therapeutic approach is to focus on the very early stage of this cascade by using a humanized anti-IgE monoclonal antibody (rhuMAb E25), which is specific for the binding sites of IgE to its high-affinity receptor (Presta et al., 1993; Kolbinger et al., 1993). Both *in vitro* and *in vivo* studies show that rhuMAb E25 is able to effectively block the binding of IgE to its high-affinity receptor without stimulating the degranulation of mast cells and basophils (Presta et al., 1993).

Several factors are critical for the success of this proposed therapy. In particular, the binding affinity between the IgE and anti-IgE antibody should favor the formation of immune complexes, and the size of the complexes should result in reasonable rates of clearance without any immune complex-mediated adverse reactions. Motivated by these considerations, the interaction between IgE and rhuMAb E25 was characterized by analytical ultracentrifugation and size exclusion chromatography. Previous size exclusion chromatography studies of a chimeric murine–human anti-IgE antibody suggested that the immune complexes formed were of limiting size, on the order of trimeric or tetrameric species (Davis et al., 1993). However, no explanation was offered as to why larger immune complexes were not formed. Analytical ultracentrifugation more clearly defines the molecular weights and structures of these complexes, as well as provides an explanation for the size limit attained.

MATERIALS AND METHODS

Materials. A humanized anti-IgE monoclonal antibody, rhuMAb E25, was constructed from the complementarity-determining regions of a murine anti-IgE monoclonal antibody and a human IgG_1 frame (Presta et al., 1993). The antibody was expressed in Chinese hamster ovary cells and was prepared by a protein A column and standard chromatographic methods (Genentech, Inc., unpublished data). Human IgE was prepared from the supernatant of the culture fluid of a human myeloma cell line, U266, using an affinity column coated with anti-IgE monoclonal antibody and regular chromatographic methods (Builder et al., in preparation). The purified concentrated protein solution was then

diluted to a concentration of 0.1 mg/mL with PBS. The diluted IgE and rhuMAb E25 solutions were then mixed at different molar ratios and analyzed by using analytical ultracentrifugation and size exclusion chromatography. For sedimentation analysis, all mixed protein solutions were incubated for at least 24 h at 4 °C before the centrifugation experiments.

Size Exclusion Chromatography. Size exclusion chromatography was performed using a Hewlett-Packard 1090 HPLC system. A Superose-6 HR 10/30 column (Pharmacia LKB Biotechnology Inc.) was equilibrated with PBS at a flow rate of 0.5 mL/min. The Bio-Rad gel filtration standard and IgM (Cappel) were used to calibrate the performance of the column throughout the analysis. Samples of rhuMAb E25 and IgE complexes were analyzed at room temperature with a mobile phase of PBS at pH 7.2. The largest complex formed by rhuMAb E25 and IgE was isolated by size exclusion chromatography and characterized by sedimentation analysis.

Sedimentation Equilibrium. The average molecular weights of rhuMAb E25, IgE, and their complexes were determined by sedimentation equilibrium analysis. Sedimentation equilibrium experiments were performed at 5000, 7000, and 10 000 rpm at 10 °C in a Beckman XLA ultracentrifuge using charcoal-filled Epon six-channel Yphantis cells (Yphantis, 1964). The concentration gradients were measured at 280 nm with a scanning absorption optical system. The sedimentation data were acquired with on-line data acquisition software (XLA, Beckman, Inc.). The attainment of an equilibrium state was verified by comparing successive scans after approximately 18 h. The partial specific volume ($\bar{v}$) of rhuMAb E25 (0.726 mL/g) was computed from its amino acid (Presta et al., 1993) and an average carbohydrate composition of 2% (Roitt et al., 1989) by using an average $\bar{v}$ (0.63 mL/g) for the typical type of N-linked carbohydrates (Shire, 1994). The value of $\bar{v}$ for IgE (0.716 mL/g) was calculated from its amino acid and carbohydrate composition (Høiland et al., 1986; Ikeyama et al., 1986). The density of PBS (ϱ = 1.006 g/mL) was measured directly with a digitized Paar density meter (DMA 35, Anton Paar K.G.). The viscosity of the buffer was also determined experimentally by using an Ubbelohde viscometer with an automated fiber optic measuring system (Lauda Viscometer C, Brinkmann, Inc.). The absorptivity of rhuMAb E25 [1.6 (mg/mL)$^{-1}$ cm^{-1}] was determined for comparison of the absorption spectrum of native protein with those of enzyme digests (Bewley et al., 1982; Gray et al., 1994), and the absorptivity of IgE [1.7 (mg/mL)$^{-1}$ cm^{-1}] was determined from its amino acid composition using a computer program (Gray et al., 1994). This program computes absorptivity values using experimentally determined spectra of model amino acids.

The data for sedimentation equilibrium were edited using a PC program, REEDIT. Data points were truncated at high concentrations (>1.5 OD) to avoid nonlinearity. The data from the very low concentration gradient around the meniscus area were also deleted because of the low signal to noise ratio. For interaction of rhuMAb E25 with IgE, models that were found to be useful included a single ideal species,

$$C(r) = \delta + C(r_0)e^{\sigma\xi} \qquad (1)$$

an ideal heterotrimer association system,

$$C(r) = \delta + C_A(r_0)e^{\sigma_A\xi} + C_B(r_0)e^{\sigma_B\xi} + \\ C_A(r_0)C_B(r_0)e^{\sigma_{AB}\xi+\ln(K_a)} + \\ C_A(r_0)C_B^2(r_0)e^{\sigma_{AB_2}\xi+2\ln(K_a)} \qquad (2)$$

and a monomer–trimer irreversible association system,

$$C(r) = \delta + C_B(r_0)e^{\sigma_B\xi} + C_{AB_2}(r_0)e^{\sigma_{AB_2}\xi} \qquad (3)$$

where $C(r)$ is the total concentration at a given radius r, δ is the baseline offset, $C_A(r_0)$ and $C_B(r_0)$ are the concentrations of each component at the arbitrary reference radius r_0, $\xi = (r^2 - r_0^2)/2$, and K_a is the intrinsic association constant of monomer–trimer equilibrium. The reduced molecular weight, σ, is defined as

$$\sigma = \frac{M(1 - \bar{v}\varrho)\omega^2}{RT} \qquad (4)$$

where R is the gas constant, T is the temperature in Kelvin, $\bar{v}$ is the partial specific volume, ϱ is the buffer density, M is the molecular weight, and ω is the angular velocity. For a heteroassociation system, σ from a nonlinear fitting of eq 1 gives the weight-average reduced molecular weight (Yphantis, 1960). σ_A and σ_B are the reduced molecular weights of components A and B. The reduced molecular weight of dimer, σ_{AB}, and trimer, σ_{AB_2}, are given by

$$\sigma_{AB} = \sigma_A + \sigma_B \qquad (5)$$

$$\sigma_{AB_2} = \sigma_A + 2\sigma_B \qquad (6)$$

while the partial specific volumes of complexes are set equal to the average partial specific volume of their components A and B by using

$$\bar{v}_{A_nB_m} = \frac{nm_A\bar{v}_A + mM_B\bar{v}_B}{nM_A + mM_B} \qquad (7)$$

where n and m are derived from the stoichiometry of the complex.

The edited data were analyzed as a single ideal species with the nonlinear least-squares fitting program, NONLIN (Johnson et al., 1981), and the ideal n-mer association systems with a commercial PC graphic program, Origin. The baseline offsets were considered in all the fitting procedures. There were no significant differences in terms of fitting parameters in fits with or without considering the baseline offsets. The association constants were determined from the best-fit values of the model, returned by nonlinear least-squares regression. The molar association constants were converted from absorbance units to molarity units by using

$$K_a = K_{ob}\sqrt{\left(\frac{M_AM_B^2}{M_{AB_2}}\right)\left(\frac{\epsilon_A\epsilon_B^2}{\epsilon_{AB_2}}\right)} \qquad (8)$$

where K_a and K_{ob} are the intrinsic association constants on the molar concentration scale and absorbance scale respectively, M_A, M_B, and M_{AB_2} are the molecular weights of components A and B and complex AB_2, while ϵ_A, ϵ_B, and ϵ_{AB_2} are the absorptivity values of components A and B and their complex.

Sedimentation Velocity. Sedimentation velocity experiments were also conducted in a Beckman XLA ultracentrifuge. Sedimentation velocity analyses were carried out at

Table 1: Sedimentation Characterization of IgE, rhuMAb E25, and the Complexes

molecules	experimental $S_{20,w}$[a]	literature $S_{20,w}$[b]	experimental MW[c]	literature or calculated MW
IgE	8.2 ± 0.1	8.0	$193\,000 \pm 10\,000$	$190\,000$[d]
rhuMAb E25	7.1 ± 0.1	7.0	$148\,000 \pm 12\,000$	$148\,000$[d]
IgE:rhuMAb E25 (10:1)	13.8 ± 0.2	NA	$271\,000$[e] $\pm 26\,000$	$270\,000$[f]
IgE:rhuMAb E25 (1:10)	13.4 ± 0.2	NA	$256\,000$[e] $\pm 24\,000$	$263\,000$[f]
larger complex (IgE−rhuMAb E25)	21.0 ± 0.2	NA	$1\,056\,000$[g] $\pm 61\,000$	$1\,023\,000$[h]

[a] Sedimentation coefficient at standard condition of water at 20 °C, determined by sedimentation velocity. [b] Literature values of sedimentation coefficient or molecular weight (Roitt et al., 1989). [c] Weight-average molecular weight, determined by sedimentation equilibrium. [d] Molecular weights from their amino acid and average carbohydrate compositions (see Materials and Methods). [e] Weight-average molecular weights of IgE and rhuMAb E25 mixtures. [f] Calculated weight-average MW of IgE and rhuMAb E25 mixtures, determined from differential sedimentation coefficient distribution by integrating the peak area as the weight fraction for each species. A heterotrimer with two IgE and one rhuMAb E25 or one IgE with two rhuMAb E25 was assumed here for the calculation. [g] Weight-average molecular weight of the purified largest complex. [h] The calculated MW of the largest complex was estimated on the basis of a model of heterohexamer with three IgE and three rhuMAb E25.

60 000 rpm at 10 °C using charcoal-filled Epon 12 mm double-sector centerpieces. The moving boundary was monitored by repetitive radial scanning at a constant time interval of 1 min using the XLA UV absorption optical system.

Sedimentation velocity data from the acquisition software (XLA, Beckman, Inc.) were analyzed using the time derivative of the concentration distribution by the method of Stafford (1992) to produce the differential sedimentation coefficient distribution. The value of $g(s)$ is the derivative of $G(s)$ that gives the weight fraction of the sample having a sedimentation coefficient (S) less than or equal to a specified value of S. The $g(s)^*$ refers to the apparent value that has not yet been corrected for the effects of diffusion. In cases for which diffusion can be ignored with respect to sedimentation, $g(s)^*$ is equal to the true distribution, $g(s)$. The apparent sedimentation coefficients ($S_{10,solvent}$) at 10 °C in PBS were corrected to standard conditions in water at 20 °C ($S_{20,w}$) using the method described by Van Holde (1985).

Hydrodynamic Modeling. The hydrodynamic properties of IgG, IgE, and complexes were calculated with the conventional procedure for a bead model using the computer program HYDRO (Garcia de la Torre, 1989, 1993). The molecular models of immune complexes were constructed from the general structures of rhuMAb E25 (IgG_1) and IgE by using spheres as their building fragments. To simplify modeling of the complex, the four-sphere structure of Díaz for IgG_1 was used (Díaz et al., 1990). This model contained three spheres to describe the F_{ab} and F_c regions and another smaller sphere to represent the hinge region. The radii of the spheres and lengths of the connectors between the center of each sphere were the same as the values used by Díaz in order to reproduce the experimental data. The model of IgE is described with seven spheres (radius = 40 Å) for its F_{ab} and F_c (Baird et al., 1993). Two extra smaller spheres were included into the hinge region for flexibility. The dimension of the sphere (radius = 2.5 Å) were calculateed according to the length of IgE (top to bottom distance = 180 Å). The angle β (Table 2) between the two F_{ab} segments were set equal to 90° (Baird et al., 1993), and the bend angle α (Table 2) between the plane of the two F_{ab} arms and F_c was rotated along the hinge to yield the closest agreement to the experimental data. The estimates of hydration for IgG and IgE were assumed to be 0.3 g of H_2O/g of protein, which is consistent with the estimates for most studied serum globular proteins using microcalorimetric measurements (Mrevlishvili, 1986).

RESULTS AND DISCUSSION

Characterization of Individual Proteins. Sedimentation velocity and size exclusion HPLC analyses of IgE and rhuMAb E25 show no significant self-association of these individual proteins over the range of concentrations tested (0.05 mg/mL or 0.33 μM to 0.64 mg/mL or 4.3 μM). The sedimentation coefficients of these molecules (Table 1, Figure 1A) were in good agreement with previous analyses (Roitt et al., 1989), as well as with the computations (Table 2) from hydrodynamic modeling.

The molecular weight of rhuMAb E25 as determined by sedimentation equilibrium (Table 1) was in good agreement with the molecular weight determined from its amino acid composition. The molecular weight of IgE calculated purely from the amino acid composition was about 12% less than the molecular weight from sedimentation equilibrium. These results are consistent with the total carbohydrate contents of IgG and IgE at ~2% and ~12% by weight, respectively (Roitt et al., 1989; Ikeyama et al., 1986).

Distribution of Complex Formation by IgE and rhuMAb E25. Sedimentation analyses and size-exclusion chromatography were performed to determine complex formation by rhuMAb E25 and IgE at various molar ratios. Sedimentation velocity experiments show that IgE and rhuMAb E25 form a variety of immune complexes in PBS (Figure 1B,C). IgE monoclonal antibody has two potential binding sites for rhuMAb E25 (one on each F_c heavy chain) and, therefore, can function as a multivalent ligand. However, unlike the polyclonal anti-IgE antibody interaction with IgE, which usually results in very large complexes (unpublished data), these monoclonal antibodies only form soluble complexes of limited sizes. The sizes of these complexes demonstrate a very strong dependence on the molar ratios of the interacting components. At a molar ratio of 1:1, IgE and rhuMAb E25 predominantly resulted in the largest complex, with small amounts of intermediate complexes and IgE monomer. However, if either IgE or rhuMAb E25 was in large molar excess, only the smaller intermediate complexes were observed, while the largest complex was almost undetectable. This result suggests that the complexes formed by IgE and rhuMAb E25 at various molar ratios are likely to involve different pathways of assembly.

The weight-average molecular weights of rhuMAb E25 and IgE at different molar ratios were also measured by sedimentation equilibrium experiments (Figure 2). The distributions of average molecular weights obtained at
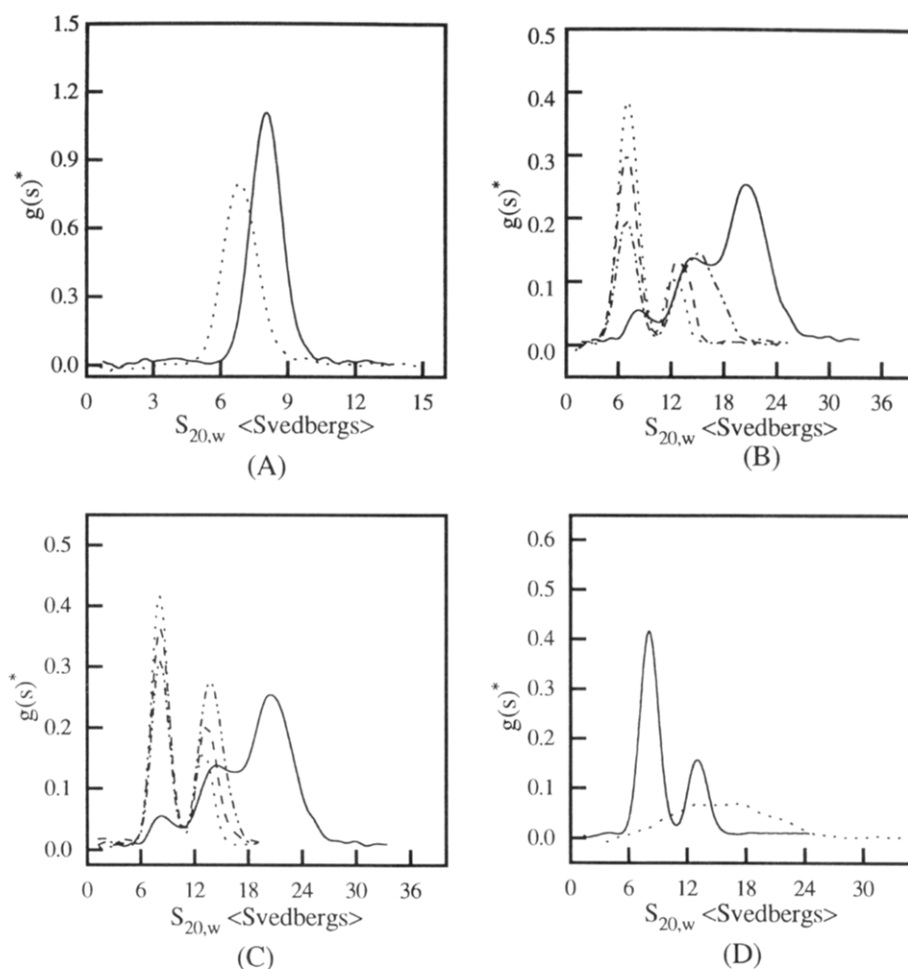
(A)

(B)

(C)

(D)

FIGURE 1: Differential sedimentation coefficient distribution of IgE (solid line) and rhuMAb E25 (dotted line) monomers at 0.64 mg/mL (A); IgE and rhuMAb E25 complexes at various molar ratios (B, C); and intermedite complex formed by IgE and rhuMAb E25 at a 10:1 molar ratio (D) in PBS at 10 °C. The molar ratios of IgE:rhuMAb E25 were as follows: (B) 1:1 (soline line), 1:3 (dash−dotted line), 1:6 (dashed line), and 1:10 (dotted line); (C) 1:1 (solid line), 3:1 (dash−dotted line), 6:1 (dashed line), and 10:1 (dotted line). The isolated intermediate complexes (dotted line) shown in (D) were collected from the mixture of IgE and rhuMAb E25 at a molar ratio of 10:1 (solid line) using size exclusion chromatography. The sedimentation coefficients have been corrected to the standard condition of water at 20 °C. No faster moving species was observed in early scanning.
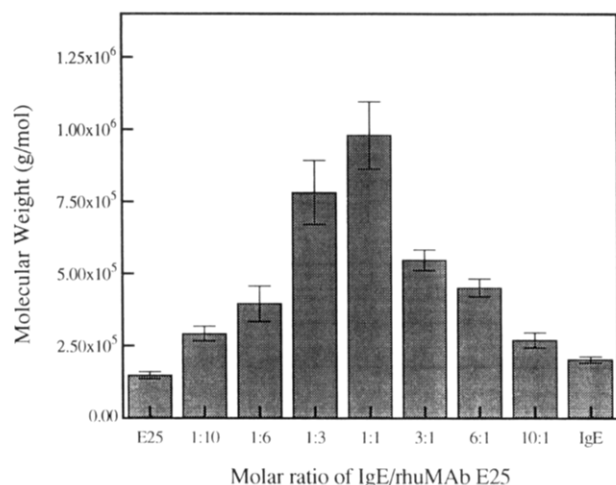

Molar ratio of IgE/rhuMAb E25

FIGURE 2: Sedimentation equilibrium analysis of IgE and rhuMAb E25 complex formation in PBS at 10 °C. The weight-average molecular weights of complexes at different molar ratios were obtained by analyzing the data from three different rotor speeds (5000, 7000, and 10 000 rpm) as a single ideal species simultaneously. The error bars correspond to a 95% confidence interval.

different molar ratios were consistent with the changes in complex sizes observed by sedimentation velocity and size exclusion chromatography (Figure 3).
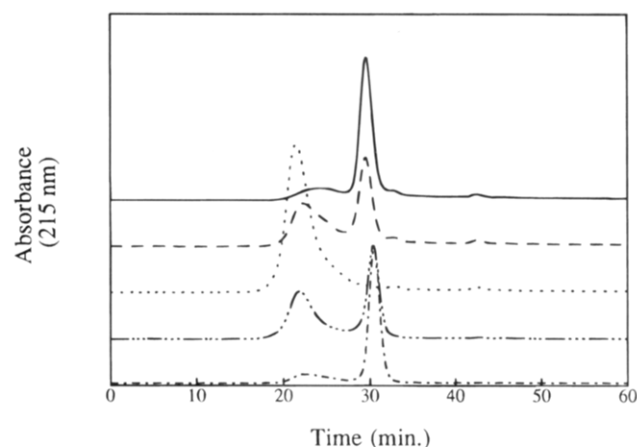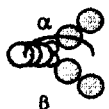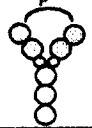

Time (min.)
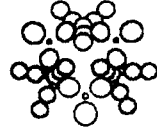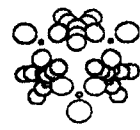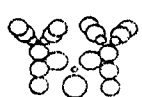
FIGURE 3: Size exclusion chromatography of IgE and rhuMAb E25 complexes at different molar ratios. The Superose-6 column was calibrated with Blue Dextran (~2 million) as a void volume marker and IgM (970 000) with Bio-Rad SEC standard for the estimation of molecular weights of complexes. The molar ratios of rhuMAb E25:IgE were 1:10 (solid line), 1:3 (dashed line), 1:1 (dotted line), 3:1 (dash−dotted line), and 10:1 (long dash−short dashed line).

Formation of the Largest Complex. The sedimentation coefficient ($S_{20,w}$) of the largest complex formed by IgE and rhuMAb E25 at a 1:1 molar ratio was determined to be 21

Table 2:   Hydrodynamic Modeling of IgG, IgE, and Complexes

Models	Ab and Complex	Experimental $S_{20,w}$	Calculated $S_{20,w}$
	Ig G	7.1 ± 0.1 s	7.1 s
	Bent Ig E 0.3g H2O/g Protein	8.2 ± 0.1 s	8.2 s
	Flat Ig E 0.2g H_2O/g Protein	8.2 ± 0.1 s	8.2 s
Hexamer with 3 IgE and 3 rhuMAb E25			
	Linear hexamer with bent IgE	21.0 ± 0.2 s	19.5 s[a]
	Linear hexamer with flat IgE	21.0 ± 0.2 s	19.5 s[a]
	Cyclic hexamer with bent IgE	21.0 ± 0.2 s	21.2 s[b]
	Cyclic hexamer with flat IgE	21.0 ± 0.2 s	21.2 s[b]
Trimer with one IgE and two rhuMAb E25			
	Trimer with Bent IgE	13.4 ± 0.2 s	13.5 s
	Trimer with Bent IgE	13.4 ± 0.2 s	13.8 s
Trimer with two IgE and one rhuMAb E25			
	Trimer with Bent IgE	13.8 ± 0.2 s	14.0 s
	Trimer with Bent IgE	13.8 ± 0.2 s	14.3 s

[a] The bent IgE in the middle of the linear hexamer has the F_{ab} arm pointing in the direction opposite to the F_{ab} of the other two IgE. The linear hexamer made of the flat IgE has the middle IgE tilted away from the plane that includes the three rhuMAb E25 and two IgE molecules at approximately of 45°, in order to avoid the overlapping of spheres. [b] Both the flat IgE and bent IgE from the cyclic hexamer were tilted away at approximately 70° from the plane that contains the three rhuMAb E25.

S by extrapolating to the standard condition of water at 20 °C (Table 1). For further characterization, the largest complex was isolated by Superose-6 size exclusion chromatography. No apparent dissociation was observed when the isolated complex was rechromatographed (data not shown), indicating that this complex is very stable.

The oligomeric state of the largest complex was revealed by sedimentation equilibrium. The best fits for the data sets were achieved by assuming a model of a single ideal species (Figure 4). The molecular weight of the largest complex was almost exactly that expected for a hexameric structure of three IgE and three rhuMAb E25 molecules (Table 1). Moreover, the average molecular weights determined were virtually the same at various rotor speeds, suggesting that the fraction collected by HPLC was homogeneous. Taken together, these results strongly suggest that the purified largest complex is dominated by a very stable hexameric form.

Interestingly, the largest complex of IgE and rhuMAb E25 was only observed around a 1:1 molar ratio. When one
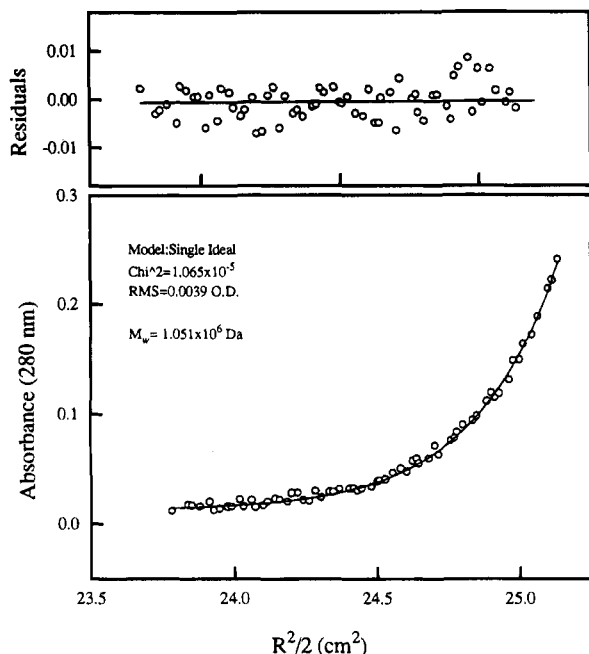
FIGURE 4: Sedimentation equilibrium analysis of the largest complex of IgE and rhuMAb E25. The data at rotor speed 5000 rpm were fit as a single ideal species (MW = 1 051 000, RMS = 0.0039 OD, and $\chi^2 = 1.07 \times 10^{-5}$) by Origin. The weight-average molecular weight of the complex was calculated by using the partial specific volume of 0.718 mL/g.

interacting component was in large molar excess, only smaller intermediate complexes were formed. One possible explanation is that the formation of the largest complex requires the simultaneous presence of both heterotrimers (two IgE with one rhuMAb E25 and one IgE with two rhuMAb E25). If either IgE or rhuMAb E25 is in large molar excess, the formation of one trimer form may be much more kinetically favored than the another trimer. The binding sites on the antibody at lower concentrations would be completely occupied by the other antibody that is present in excessive amounts. As a result, the reaction will terminate at the smaller intermediate form.

Formation of similar complexes by IgE and chimeric murine—human anti-IgE monoclonal antibodies has recently been reported by Davis et al. using size exclusion chromatography (Davis et al., 1993). In particular, these antibodies also formed complexes of limited sizes that varied with the molar ratios of the interacting antibodies. However, the largest complex size at a 1:1 molar ratio was reported to be trimeric or tetrameric, which is significantly smaller than the hexameric structures determined here by analytical ultracentrifugation. One possible reason for this discrepancy is the difference in the anti-IgE antibodies: the antibody studied by Davis et al. was a chimera, whereas ours is a humanized version. However, this may not be the correct explanation since size exclusion chromatography of complexes formed by rhuMAb E25 and IgE also suggests that the largest size complex formed is on the order of a tetramer (Figure 3). It is more likely that either interaction with the chromatographic medium or the effect of hydrodynamic shape leads to an incorrect assignment of molecular weight by the chromatographic procedure.

Intermediate Complex Formation. Sedimentation velocity experiments showed that IgE and rhuMAb E25 form a variety of intermediate complexes at different molar ratios.

At lower molar ratios (molar ratios between two interacting components < 4:1), the intermediate complexes appeared to contain a number of different sizes of oligomers (Figure 1B,C); however, at higher molar ratios (molar ratios between two interacting components > 6:1), a dominant form of complex was observed. To characterize the stoichiometry of this complex, initially we used size exclusion chromatography to isolate it from samples at high molar ratios (1:10 or 10:1) for sedimentation equilibrium characterization. Unfortunately, this intermediate was unstable when it was isolated from the excess free antibody monomer. The intermediates collected by HPLC show significantly higher values of sedimentation coefficients and molecular weights than the intermediates that were not separated by HPLC (Figure 1D). Moreover, the intermediates isolated by HPLC appeared to be very heterogeneous (Figure 1D). However, if the mixture of intermediate complexes and excess monomer was treated with a bivalent cross-linker such as DSS before chromatography, the intermediate complex peak shifted to smaller size. This shift occurred even though the uncomplexed IgE and rhuMAb E25 monomers eluted at slightly larger sizes because of the covalent attachment of the DSS cross-linker (data not shown). These results strongly suggest that the intermediate complexes are able to rearrange into larger and more stable complexes when they are separated from the excess monomer. When the IgE and rhuMAb E25 mixture was first loaded onto the HPLC column, it had a molar ratio of IgE to rhuMAb E25 of either 1:10 or 10:1. During chromatographic separation, the excess monomer, either IgE or rhuMAb E25, was separated from the complexes, thus lowing the molar ratio of the fraction containing the intermediates. At these lower molar ratios, the larger size complexes will form (Figure 1B,C). The addition of the bivalent cross-linker DSS may prevent the dissociation of intermediates and exposure of binding sites, which are required for the formation of the larger complexes. Therefore, the intermediate complex size distribution observed by size exclusion chromatography is not the same as the distribution formed in the presence of excess antibody monomers, but now represents the larger complexes after rearrangement. In contrast, in the sedimentation velocity experiment, the larger intermediate complexes always sediment in the presence of excess monomer. Since there is no real separation between the smaller antibody monomer and the larger intermediate complex, the distribution of complex observed by sedimentation velocity is more likely to reflect what happens during intermediate complex formation in solution.

Since it was not possible to isolate intermediates by size exclusion chromatography, an alternate strategy was used to estimate the size of the predominant species present at high IgE:rhuMAb E25 molar ratios of either 1:10 or 10:1. A weight-average molecular weight was first estimated by analyzing the sedimentation equilibrum data with a single ideal species model. Then the amounts of excess antibody and main intermediate complex formed at the high molar ratios were estimated by integrating the peaks from the sedimentation coefficient distribution profile. Finally, by assigning a putative trimeric size for the intermediate complex, the weight-average molecular weights of IgE and rhuMAb E25 mixtures at high molar ratios were calculated. These computed weight-average molecular weights for a heterotrimeric model with two IgE and one rhuMAb E25
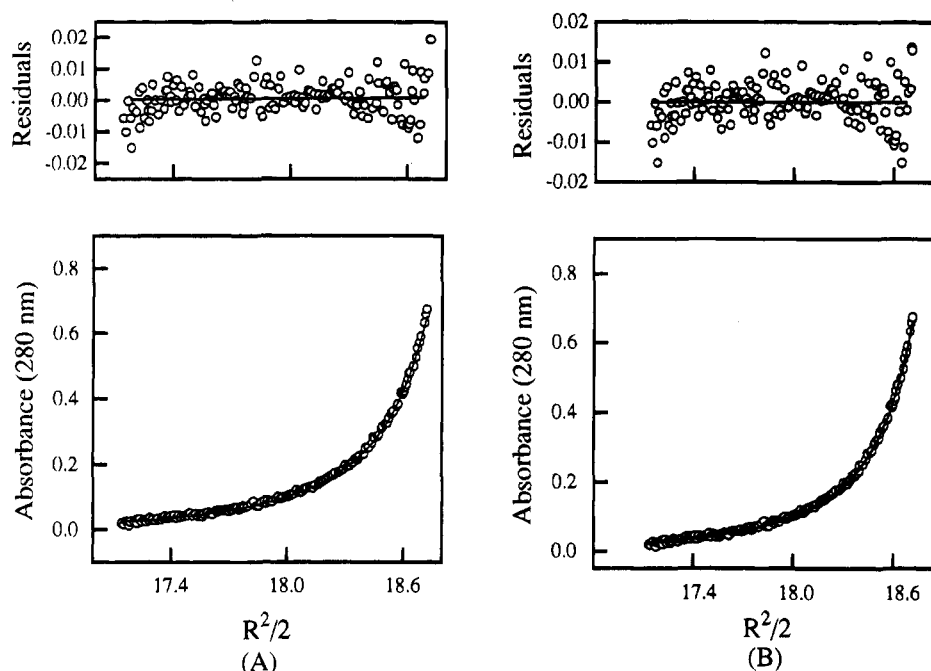
FIGURE 5: Nonlinear least-squares analysis of sedimentation equilibrium data for IgE and rhuMAb E25 at a molar ratio of 1:10. Data at rotor speed 10 000 rpm were fit either as a monomer—trimer reversible association model (panel A, $K_a = 1 \times 10^7$ M^{-1}, RMS = 0.0053 OD, and $\chi^2 = 2.72 \times 10^{-5}$) or as a monomer—trimer irreversible heteroassociation model (panel B, RMS = 0.0044 OD and $\chi^2 = 2.63 \times 10^{-5}$). The K_a is the intrinsic association constant of monomer—trimer association.

(or one IgE and two rhuMAb E25) were in good agreement with the experimentally determined values (Table 1). These results suggest that the distribution of intermediate complexes formed at high molar ratios is likely to be dominated by a heterotrimer.

For further verification of the presence of trimeric intermediate structures, sedimentation equilibrium ultracentrifugation data for the IgE and rhuMAb E25 mixtures at molar ratios of 1:10 or 10:1 were analyzed using numerous models. Models that invoked the formation of tetramer or dimer always failed to give reasonable fits to the data, whereas the model that consistently gave the best fit was for heterotrimer association (discussed further in the next section). This result is consistent with our observation of heterotrimer formation from the weight-average molecular weight comparison.

Affinity of IgE and rhuMAb E25. The association constant for IgE and rhuMAb E25 interaction was estimated by using sedimentation equilibrium. To simplify the analysis, samples from the IgE and rhuMAb E25 mixtures at molar ratios of 1:10 or 10:1 were used. As discussed previously, under these conditions, the IgE and rhuMAb E25 interact reversibly and the distribution of complexes appears to be dominated by excess monomer antibody and a heterotrimer complex. A monomer—trimer reversible heteroassociation model with an intrinsic association constant (as defined by eqs 2 and 8) on the order of 10^7 M^{-1} provided an adequate fit to the data (Figure 5A). However, if the intrinsic association constant for this model was held at 10^9 M^{-1}, then the resulting fit was not statistically different from the fit that resulted in an intrinsic association constant of 10^7 M^{-1}. If a large K_a was used as an initial guess ($\sim 10^9$ M^{-1}) and allowed to float, then the nonlinear regression analysis converged slowly and resulted in very large association constants with large errors. This suggests that the nonlinear fitting algorithm is unable to distinguish the best fit for the association constant under

these conditions. Additional experiments using plasmon surface resonance technology (BIAcore, Pharmacia) and radioimmunoassays (J. Fox and G. Meng, personal communication) suggest that IgE and rhuMAb E25 interact strongly with a K_d in the sub-nanomolar range. To test the possibility of a tight association between IgE and rhuMAb E25, an ideal non-interacting two-species model consisting of a monomer and a heterotrimer was tested. As shown in Figure 5B, this model provides an excellent fit by all the criteria that can be applied (Johnson et al., 1981). These results suggest that the interaction of IgE and rhuMAb E25 is very strong and favors formation of the trimer. It is likely that, even at the lowest concentration (0.1 mg/mL or 0.33 μM) examined in our experiments, only a very small fraction of the heterotrimer is dissociated. Therefore, the affinity constants shown in Figure 5A may only reflect a lower limit for the association constant. A more accurate determination of such a high-affinity interaction requires that data be obtained at far lower protein concentrations ($<\mu$g/mL) than can be monitored by the current XLA absorption optical system. Taken together, however, these observations strongly support the notion that IgE and rhuMAb E25 have a very high affinity.

Hydrodynamic Struture of Antibody and Complex. Hydrodynamic properties such as sedimentation or frictional coefficients essentially depend on the overall conformation of the macromolecules. The calculation of sedimentation coefficients and other solution properties with the bead model treatment has been successfully used to estimate the structure and conformation of immunoglobulin and several other multisubunit macromolecules (Garcia de la Torre, 1992).

Previously Baird et al. showed that IgE had a bent structure by using fluorescence resonance energy transfer techniques (Baird et al., 1993). A similar conclusion was also reached by Davis et al. (1990) using a bead model treatment. Hydrodynamic computations using a nine-sphere bead model

(Table 2) are consistent with the assignment of a bent conformation for IgE in solution. By assuming a hydration of 0.3 g of H_2O/g of protein, a bent angle of approximately $110°$ (defined as angle α in Table 2) and an F_{ab} angle of $90°$ (defined as β in Table 2) yield a calculated value of 8.2 S, which is in excellent agreement with the experimentally determined value. However, this agreement should be interpreted with caution. The computed value for α will be quite dependent on the assumption of hydration, as well as the value assumed for β. In fact, a planar structure represented by a nine-bead model also yields excellent agreement with experiment, using a hydration of 0.2 g of H_2O/g of protein. Although uncertainties in hydration or exact choice of bead model will influence the computations, hydrodynamic modeling is still useful in evaluating the types of structures that IgE and rhuMAb E25 may form. As shown in Table 2, the theoretical sedimentation coefficients using a nine-bead model for a linear or cyclic structure were independent of whether the IgE was bent or planar. Thus, if it is assumed that IgE does not undergo a large conformational change after binding to rhuMAb E25, then the computations may be insensitive to the exact choice of hydration. This is not an unreasonable assumption on the basis of the similarity of the IgE conformation in solution compared to the conformation when bound to receptor (Zheng et al., 1992). For the largest complex, the calculated value for a cyclic structure is in very good agreement with the experimental data, while the sedimentation coefficient calculated from the structure containing a linear arrangement of antibodies is significantly smaller than the experimental value. This suggests that the largest complex formed by IgE and rhuMAb E25 may contain a cyclic or near-cyclic structure.

A preliminary low-resolution electron microscopy study also shows that the largest complex formed by IgE and rhuMAb E25 may have a ringlike structure (M. Siegel, personal communication). Since both IgE and rhuMAb E25 are bivalent molecules, potentially they are able to form much larger complexes. However, in a closed ringlike structure, all the binding sites in the complex either will be fully satisfied or will be sterically inaccessible if the ring is nearly closed. Therefore, the reaction has been terminated at the hexamer level.

It should be noted that hydrodynamic modeling of immune complexes peformed here has not considered the flexibility of IgE and IgG, nor were many of the potential arrangements of complexes fully explored. This may partly account for the difference between experimental and calculated values. However, data from hydrodynamic modeling at least are consistent with the hypothesis that the largest complex of IgE and rhuMAb E25 may have a near-cyclic structure.

The sedimentation coefficients of the heterotrimers with bent IgE were also calculated (Table 2). The IgE orientation relative to rhuMAb E25 has a small effect on the computed sedimentation coefficient. The model with the F_c portions of IgE and rhuMAb E25 oriented in the same plane gives a slightly larger sedimentation coefficient than the model with one IgE tilted away from the rhuMAb E25 (about $70°$ for trimer with one IgE and two rhuMAb E25 or $40°$ for trimer with one rhuMAb E25 and two IgE). The latter model may be the preferred structure, since there is closer agreement between the computed and experimentally determined values.

At any rate, the difference between these models is small, and thus these results are consistent with the assignment of trimeric structures as predominant intermediates in the association pathway.

CONCLUSIONS

Analytical sedimentation equilibrium and velocity analyses have been used to characterize the size distributions of complexes formed by a humanized anti-IgE monoclonal antibody and human IgE. Although an accurate K_a value could not be determined for the interaction, it appears to be in the range ($<$nM) expected for normal antibody interactions. The bivalent nature of both antibodies should result in large complexes, but even though the size distribution was greatly dependent on the molar ratio of the two antibodies, a hexamer was the maximum size observed at around a 1:1 molar ratio. Sedimentation velocity and hydrodynamic modeling analyses suggest that the largest complex may contain a nearly cyclic structure. This model provides an explanation for why such a complex does not interact further to form larger oligomers. Moreover, characterization of the intermediates at high molar ratios suggests a plausible model for the assembly of the hexamer through two different heterotrimers. The limited size of the complex formed could have important ramifications in regard to the clearance rate for the immune complex. In particular, an increased residence time for the complex within the body may affect the potential binding of IgE to its high-affinity receptor. In essence, the relative binding of IgE to rhuMAb E25 versus high-affinity F_c receptor will be critical for the success of the proposed allergy therapy. Studies are currently underway to further characterize interactions between free IgE and the IgE bound in immune complexes with the high-affinity F_c receptors.

REFERENCES

Baird, B., Zheng, Y., & Holowka, D. (1993) *Acc. Chem. Res. 26*, 428–434.

Bewley, T. A. (1982) *Anal. Biochem. 123*, 55–65.

Davis, F. M., Gossett, L. A., Pinkston, K. L., Liou, R. S., Sun, L. K., Kim, Y. W., Chang, N. T., Chang, T. W., Wagner, K., Bews, J., Brinkmann, V., Towbin, H., Subramanian, N., & Heusser, C. (1993) *Springer Semin. Immunopathol. 15*, 51–73.

Davis, K. G., Glennie, R., Harding, S. E., & Burton, D. R. (1990) *Biochem. Soc. Trans. 18*, 935–936.

Díaz, F. G., Iniesta, A. & Garcia de la Torre, J. (1990) *Biopolymers 30*, 547–554.

Garcia de la Torre, J. (1989) in *Dynamic Properties of Biomolecular Assemblies* (Harding, S. E., & Rowe, A., Eds.) pp 1–41, Royal Society of Chemistry, Cambridge, UK.

Garcia de la Torre, J. (1992) in *Analytical Ultracentrifugation in Biochemistry and Polymer Science* (Harding, S., & Rowe, A., Eds.) pp 359–393, The Royal Society of Chemistry, Cambridge, UK.

Garcia de la Torre, J., Navarro, S., Lopez Martinez, M. C., Diaz, F. G., & Lopez Cascales, J. J. (1993) *Biophys. J. 67*, 530−531.

Gray, R., Stern, A., Bewley, T. A., McRorie, D., Voelker, P., Liu, J., & Shire, S. (1994) *Pharm. Res. 11*, 76.

Høiland, H. (1986) in *Thermodynamic Data for Biochemistry and Technology* (Hinz, H. J., Ed.) pp 99−125, Springer-Verlag, Berlin.

Ikeyama, S., Nakagawa, S., Arakawa, M., Sugino, H., & Kakinuma, A. (1986) *Mol. Immunol. 23*, 159−167.

Johnson, M. L., Correia, J. C., Yphantis, D. A., & Halvorson, H. R. (1981) *Biophys. J. 36*, 578−588.

Kolbinger, F., Saldanha, J., Hardman, N., & Bendig, M. M. (1993) *Protein Eng. 6*, 971−980.

Mrevlishvili, G. M. in *Thermodynamic Data for Biochemistry and Technology* (Hinz, H. J., Ed.) pp 165, Springer-Verlag, Berlin.

Presta, L. G., Lahr, S. J., Shields, R. L., Porter, J. P., Gorman, C. M., Fendly, B. M., & Jardieu, P. (1993) *J. Immunol. 151*, 2623−2632.

Roitt, I., Brostoff, J., & Male, D. (1989) in *Immunology*, 2nd ed. (Roitt, I., Brostoff, J., & Male, D., Eds.) pp 5.1−5.11, Harper & Row, New York.

Shire, S. J. (1994) in *Modern Analytical Ultracentrifugation* (Schuster, T. M., & Laue, T. M., Eds.) pp 261−291, Birkhäuser, Boston.

Stafford, W. F. (1992) in *Analytical Ultracentrifugation in Biochemistry and Polymer Science* (Harding, S., & Rowe, A., Eds.) pp 359−393, The Royal Society of Chemistry, Cambridge, UK.

Van Holde, K. E. (1985) in *Physical Biochemistry*, 2nd ed. (Van Holde, K. E., Ed.) pp 110−136, Prentice-Hall Inc., Englewood Cliffs, CA.

Yphantis, D. A. (1960) *Ann. N.Y. Acad. Sci. 88*, 586−601.

Yphantis, D. A. (1964) *Biochemistry 3*, 297−317.

Zheng, Y., Shopes, B., Holowka, D., & Baird, B. (1992) *Biochemistry 31*, 7446−7456.